

1 Binding and Relocalization of PKR by Murine Cytomegalovirus

2

3 Stephanie J. Child¹ and Adam P. Geballe^{1,2*}

4

5 ¹Divisions of Human Biology and Clinical Research, Fred Hutchinson Cancer Research
6 Center, Seattle, WA 98109, and ²Departments of Medicine and Microbiology, University
7 of Washington, Seattle, WA 98115

8

9 PKR binding and relocalization by MCMV

10

11 *Corresponding author.

12 Adam P. Geballe

13 Division of Human Biology

14 Fred Hutchinson Cancer Research Center

15 1100 Fairview Ave N

16 MS C2-023

17 Seattle, WA 98109-1024

18 Phone (206) 667-5122

19 Fax (206) 667-6523

20 Email:ageballe@fhcrc.org

21 Word counts:

22 Abstract - 229 words

23 Text - 5762

24 **ABSTRACT**

25 Many viruses have evolved mechanisms to evade the repression of translation
26 mediated by protein kinase R (PKR). In the case of murine cytomegalovirus (MCMV),
27 the protein products of two essential genes, m142 and m143, bind to dsRNA and block
28 phosphorylation of PKR and eukaryotic initiation factor 2 α . A distinctive feature of
29 MCMV is that two proteins are required to block PKR activation whereas other viral
30 dsRNA-binding proteins that prevent PKR activation contain all the necessary functions
31 in a single protein. In order to better understand the mechanism by which MCMV evades
32 the PKR response, we investigated the associations of pm142 and pm143 with each other
33 and with PKR. Both pm142 and pm143 interact with PKR in infected and transfected
34 cells. However, the ~200 kDa pm142:pm143 complex that forms in these cells does not
35 contain substantial amounts of PKR, suggesting that the interactions between
36 pm142:pm143 and PKR are unstable or transient. The stable, soluble pm142:pm143
37 complex appears to be a heterotetramer consisting of two molecules of pm142 associated
38 with each other and each one binding to and stabilizing a monomer of pm143. MCMV
39 infection also causes relocalization of PKR into the nucleus and to an insoluble
40 cytoplasmic compartment. These results suggest a model in which the pm142:pm143
41 multimer interacts with PKR and causes its sequestration in cellular compartments where
42 it is unable to shut off translation and repress viral replication.

43 **INTRODUCTION**

44 As a consequence of the threat viruses pose to the survival and fitness of their
45 hosts, an array of cellular defenses have evolved to repress viral infection. In mammals,
46 the interferon system mediates multi-faceted innate immune responses to viral infections
47 (25). Among the important effectors of this system is the interferon-stimulated double
48 stranded RNA (dsRNA)-activated protein kinase R (PKR). dsRNA, which is produced
49 during many viral infections (29), binds to PKR, causing a conformational change,
50 dimerization, and autophosphorylation followed by phosphorylation of the alpha subunit
51 of initiation factor 2 (eIF2 α). Phosphorylated eIF2 α inhibits the activity of the guanine
52 nucleotide exchange factor eIF2B, resulting in repression of translation initiation (8).

53 Because viral replication depends on ongoing translation, viruses have evolved a
54 variety of mechanisms for evading the PKR response (22). One such mechanism utilizes
55 virally encoded dsRNA-binding proteins such as the E3L protein of vaccinia virus and
56 the NS1 protein of influenza virus. The observation that vaccinia virus lacking E3L
57 (VV Δ E3L) has a very limited host range in cell culture and is avirulent in animals but
58 does replicate in PKR-deficient cells illustrates the importance of blocking the PKR
59 response (3, 30, 31). Many viral dsRNA-binding proteins form homodimers and bind to
60 PKR, but the relative contributions of the various interactions to anti-PKR functions vary.
61 For example, in the case of E3L, binding to and sequestering dsRNA may be sufficient to
62 prevent PKR activation (5), while in the case of NS1, direct binding to PKR appears to be
63 more critical than binding to dsRNA (20).

64 In previous studies, we identified dsRNA-binding proteins encoded by two β
65 herpesviruses, human cytomegalovirus (HCMV) and murine cytomegalovirus (MCMV)

66 (6, 7). The TRS1 and IRS1 genes of HCMV each encode proteins that block PKR
67 activation by a mechanism that appears to depend on binding to both dsRNA and PKR
68 (10, 11). These proteins also have the unusual property that they cause accumulation of
69 PKR in the nucleus.

70 In the case of MCMV, the m142 and m143 genes function by blocking PKR
71 activation. Valchanova and coworkers reported that the failure of mutant viruses lacking
72 either m142 or m143 to replicate is linked to activation of PKR and inhibition of protein
73 synthesis (27). We found that the protein products of these two genes (pm142 and
74 pm143) co-immunoprecipitate in infected cells and function together to bind dsRNA and
75 to enable replication of VV Δ E3L (7). Thus, the MCMV system differs from other viral
76 systems studied thus far in that two different proteins are required to block PKR
77 activation.

78 The limited understanding of how dsRNA binding proteins actually block PKR
79 function coupled with the unusual features of the MCMV system led us to undertake
80 studies aiming to clarify the interactions among pm142, pm143 and PKR. We found that
81 like other well-studied viral dsRNA binding proteins, pm142 and pm143 each can bind to
82 PKR. Pm142 and pm143 appear to form a stable soluble heterotetrameric complex,
83 which, interestingly, does not contain substantial amounts of PKR. Similar to HCMV,
84 MCMV infection also causes relocalization of PKR to the nucleus, as well as to insoluble
85 cytoplasmic complexes. These results suggest a model in which interaction with pm142
86 and pm143 results in PKR sequestration into compartments where it is unable to shut off
87 protein synthesis.

88

89 **MATERIALS and METHODS**

90 **Cells, virus, and infections.** NIH 3T3 cells, PKR null mouse fibroblasts (provided by
91 Bryan Williams, Cleveland Clinic Foundation), and HeLa cells were maintained in
92 Dulbecco's modified Eagle's medium supplemented with 10% NuSerum (Collaborative
93 Biomedical) as previously described (6). MCMV strain K181 and MCMV MC.55, a
94 recombinant of a strain derived from K181 that expresses green fluorescent protein (GFP)
95 (provided by Jeff Vieira, University of Washington (28)) were propagated in NIH 3T3
96 cells. Infections were performed at a multiplicity of infection (MOI) of 3.

97

98 **Plasmids.** The plasmid pCS2+BirA which expresses *E. coli* biotin ligase was obtained
99 from Bruce Clurman (Fred Hutchinson Cancer Research Center). All other expression
100 constructs used in these experiments were cloned into the pcDNA3.1/V5-His-TOPO
101 vector (Invitrogen).

102 Plasmid pEQ1100, which expresses EGFP with a C-terminal biotinylation signal
103 and adjacent 6 x His tag (hereafter designated by -B and -H, respectively) was
104 previously described (7). The plasmid pEQ1068 (TRS1[1-738]-B-H) was constructed by
105 inserting primers encoding a biotinylation signal (7) into the *XhoI* and *XbaI* sites of
106 pEQ979 (10).

107 Construction of pEQ1073 (m142-B-H) was previously described (7). pEQ1163
108 (m142-B) was derived from pEQ1073 by digestion with *PmeI* and *AgeI*, blunting with
109 Klenow, and religating to remove the His tag. pEQ1063 (m142-H) was made by
110 amplification of pEQ985 (7) using oligos #461 (ACCATGGACGCCCTGTGCGC) and
111 #548 (GTCGTCATCGTCGGCGTCCGC) and cloning into the TOPO vector.

112 PEQ1109 (m143-H) was made by amplification of pEQ939 (7) using oligos #410
113 (ACCATGTCTTGGGTGACCGGAGAT) and #596 (CGCGTCGGTCGCTCTCTCGT)
114 and cloning into the TOPO vector . The m143 ORF was removed from pEQ1109 by
115 digestion with *HindIII* and *EcoRV* and cloned into pEQ1068 after digestion with the
116 same enzymes to construct pEQ1126 (m143-B-H). PEQ1164 (m143-B) was derived
117 from pEQ1126 by digestion with *PmeI* and *AgeI*, blunting, and religating.

118

119 **Transient transfection.** Sub-confluent HeLa cells in 12 well plates were transfected
120 with plasmid DNA using Lipofectamine 2000 reagent (Invitrogen) according to the
121 manufacturer's instructions. Biotin (25 μ M) was added to the medium following
122 transfection. At 24 to 48 h post-transfection the cells were washed with PBS at 4°C then
123 lysed in 300 μ l of RIPA buffer (50 mM Tris-HCl (pH 7.5), 1% Triton X-100, 0.2% SDS,
124 1% NaDOC) containing 250 mM NaCl. After reserving a portion for subsequent
125 analysis, the resulting lysates were used for binding to avidin as described below.

126

127 **Immunoprecipitation, avidin agarose pull-down, and immunoblot analyses.** For co-
128 immunoprecipitation analyses, NIH 3T3 cells in 6 well plates were either mock-infected
129 or infected with MCMV MC.55. At 48 h post-infection the cells were washed twice with
130 PBS (4°C), then lysed in 300 μ l of NP-40 lysis buffer (50 mM Tris.Cl (pH 7.5), 150 mM
131 NaCl, 1% NP-40). The cells were incubated on a rotator for 20 min., then clarified by
132 centrifugation at 16,000 x g for 10 min. at 4°C. 3% of the sample was saved for
133 assessing protein expression in the lysates. The remaining supernatants were transferred
134 to new tubes, and 5 μ l of the indicated rabbit polyclonal antiserum (pre-immune, anti-

135 m142, or anti-m143; provided by Laura Hanson and Ann Campbell, Eastern Virginia
136 Medical School (12)) was added. After 1-2 h on the rotator, protein A sepharose was
137 added to each tube, and rotation was continued for ~ 4 h. The samples were washed three
138 times with NP-40 lysis buffer, followed by separation on 10% polyacrylamide gels and
139 transfer to polyvinylidene difluoride (PVDF) membranes by electroblotting. The
140 membranes were probed with a mixture of m142 and m143 antisera or with mouse
141 monoclonal antibody PKR (B-10) (#sc-6282, Santa Cruz Biotechnology).

142 For avidin (AV) agarose binding assays, transfected cell lysates were incubated
143 with immobilized avidin (PIERCE) for 2-4 h, washed four times, then immunoblotted as
144 described above. Blots were probed with either Penta-His antibody (QIAGEN) or avidin-
145 AP (Avidx-AP conjugate; Applied Biosystems) according to the manufacturer's
146 recommendations.

147 For all immunoblot analyses, proteins were detected using the Western-Star™
148 chemiluminescent detection system (Applied Biosystems) according to the
149 manufacturer's recommendations. Silver staining was performed using the
150 SilverQuest™ silver staining kit (Invitrogen) according to the manufacturer's
151 recommendations.

152

153 **Metabolic labeling.** For pulse-chase analysis, HeLa cells were transfected as described
154 above with pCS2+BirA and either m143-B-H alone, or m143-B-H and m142-H. 24 h
155 later, the cells were labeled for 1 h with 100 µCi/ml [³⁵S]-methionine (Easytag™ express
156 protein labeling mix, PerkinElmer) and, after washing twice, chased by addition of
157 medium containing 1 mM cold methionine. At the indicated times post-chase the cells

158 were lysed with 300 μ l of RIPA buffer containing 250 mM NaCl, and the resulting
159 lysates incubated in the presence of AV-agarose as described above. The resulting
160 samples were separated on 10% polyacrylamide gels, dried, and subjected to
161 phosphorimager analysis on a Typhoon Trio multi-mode imager.

162

163 **Cell fractionation.** For glycerol gradient fractionation of infected cells, 100 mm dishes
164 of NIH 3T3 cells were infected with MCMV MC.55. At 48 h post-infection the cells
165 were scraped into PBS, pelleted, then resuspended in 250 μ l of cell fractionation buffer
166 (20 mM Hepes (pH 8.0), 150 mM NaCl, 1.5 mM $MgCl_2$, 1 mM DTT, 1% NP-40, 1 mM
167 benzamidine, 10% glycerol). The samples were incubated for 30 min., 4°C on a rotator,
168 then clarified by centrifugation (16,000 x g). Supernatants were separated on 5 ml 15-
169 35% glycerol gradients at 237,000 x g, 17 h, 4°C. Fractions were collected from the
170 bottom of the gradients and separated on 10% polyacrylamide gels, transferred to PVDF,
171 probed with a mixture of m142 and m143 antisera, then stripped and re-probed with anti-
172 PKR antiserum. Molecular weight standards were centrifuged on parallel gradients, and
173 their distribution was determined by polyacrylamide gel electrophoresis and Coomassie
174 blue staining.

175 Similar glycerol gradient fractionation of transfected cells was performed after
176 transfection of plasmids expressing m142-B-H and m143-B-H into HeLa cells. Lysates
177 prepared at 24 h post-transfection were analyzed as described for infected cells, except
178 that the PVDF membrane was probed with avidin-AP for protein detection.

179 Nuclear- and cytoplasmic-enriched fractions were prepared from 100 mm dishes
180 of NIH 3T3 cells after mock-infection or infection with MCMV MC.55. At 24, 48, and

181 72 h post-infection, the cells were washed with PBS and lysed with 1 ml of cell
182 fractionation buffer (see above). The lysates were transferred to 1.5 ml microfuge tubes,
183 and placed on a rotator at 4°C for 30 min. The samples were then centrifuged at 1000 x
184 g, 5 min., 4°C, and the supernatant (cytoplasmic-enriched fraction) removed carefully
185 without disturbing the pellet. The pellet fraction was then gently resuspended in 0.5 ml
186 of fractionation buffer, microfuged as before, and the remaining pellet (nuclear-enriched
187 fraction) resuspended in 60 µl of 2% SDS and sonicated to shear DNA. Equal amounts
188 of protein were separated on 10% polyacrylamide gels, transferred to PVDF, and
189 immunoblotted with the following antisera according to the manufacturer's
190 recommendations: PKR (B-10), lamin A/C (#2032, Cell Signaling), calnexin (#610523,
191 BD Transduction Laboratories), β-actin (#A2066, Sigma). and a mixture of m142 and
192 m143 antisera.

193

194 **Immunofluorescence.** NIH 3T3 cells or PKR null mouse fibroblasts grown on glass
195 coverslips were mock-infected or infected with MCMV K181. At 48 h post-infection the
196 cells were washed three times with PBS (4°C), fixed in 100% MeOH at -20°C for 5 min.,
197 then washed again with PBS. The coverslips were blocked with 5% normal goat serum
198 for 1 h, then incubated for 1 h with PKR (B-10) antibody or an anti-β-Gal antibody
199 (Promega) that served as an IgG2a isotype control. The coverslips were washed three
200 times with PBS, then incubated with FITC-conjugated anti-mouse secondary antibody
201 (SIGMA) for 1 h in the dark. After washing the cells three times with PBS they were
202 incubated with Hoechst 33342 (5 µg/ml; Invitrogen) for 5 min., washed twice with PBS,
203 then mounted on slides using ProLong Gold anti-fade mounting medium (Invitrogen).

204 All incubations were performed at room temperature. The samples were analyzed using a
205 Deltavision RT Wide-field Deconvolution Microscope (Applied Precision, Inc.).

206

207 **RESULTS**

208 **pm142 and pm143 form a complex that binds to PKR in MCMV-infected cells.**

209 Several viral proteins that block PKR activation bind to both dsRNA and PKR (4, 5, 10,
210 11, 16, 20, 24). We have shown that MCMV pm142 and pm143 together bind to dsRNA
211 and block PKR activation (7). Therefore, as a next step in elucidating the mechanism by
212 which pm142 and pm143 function, we investigated whether they also physically
213 associate with PKR.

214 First, we infected NIH 3T3 cells with MCMV and at 48 h post-infection prepared
215 lysates. After immunoprecipitation with pre-immune serum or antisera specific for either
216 pm142 or pm143, we analyzed the precipitated proteins by immunoblot analyses using
217 either a mixture of rabbit anti-m142 and anti-m143 antisera or with a mouse monoclonal
218 antibody directed against PKR (Fig. 1). Although the immunoglobulin heavy chain
219 partially obscured the pm142 band following precipitation of MCMV-infected lysates
220 with anti-m142 or anti-m143 antiserum, these experiments confirmed that pm142 and
221 pm143 form a complex as previously reported (7). Also, as noted previously, anti-m143
222 appeared to precipitate more pm142 compared to the amount of pm143 precipitated by
223 anti-m142 (compare lanes 7 and 8 in Fig. 1A). Importantly, pm142 and pm143 antisera
224 each precipitated PKR while preimmune serum did not (Fig 1B). The amount of PKR
225 that co-immunoprecipitated with pm142 or pm143 was relatively small, suggesting the
226 possibility that only a minority of PKR in the cell is associated with these two proteins

227 (see below). As expected, pm142, pm143 and PKR were absent from precipitates from
228 mock-infected cell lysates after precipitation with the same antisera. Thus, PKR
229 associates with pm142 and pm143 in MCMV-infected cells.

230

231 **pm142 and pm143 each bind to PKR in transfected HeLa cells.** In order to determine
232 which of the MCMV proteins (pm142, pm143, or both) associates with PKR, we used an
233 AV-agarose pull-down system as described in Materials and Methods. This system takes
234 advantage of the high affinity of the biotin-avidin interaction and eliminates background
235 resulting from the immunoglobulin heavy chain. The plasmids used in these assays
236 expressed proteins that were either His-tagged (designated pm142-H, for example), or
237 contained a 14 amino acid biotinylation signal in addition to the His tag (e.g. pm142-B-
238 H). When co-transfected into cells along with a plasmid containing the *E. coli* biotin
239 ligase (BirA) gene and incubated in the presence of 25 μ M biotin, biotin is efficiently
240 added to a lysine residue in the biotinylation signal of signal-tagged proteins (2).

241 For these analyses, we transfected HeLa cells with various combinations of
242 expression plasmids, prepared lysates at 48 h post-transfection, and detected proteins
243 present in the total lysates and in the fractions that bound to AV-agarose by assays using
244 anti-His or avidin-AP. When probed with anti-His antibody, all of the His-tagged proteins
245 were detected in the lysates (Fig. 2A, top panel). Consistent with the known interactions
246 of pm142 and pm143, both proteins were detected in the AV bead-bound fractions when
247 either one was biotinylated (Fig 2A, bottom panel, lanes 2 and 3), while neither protein
248 bound to EGFP-B-H (lanes 7 and 8), even on a longer exposure (data not shown).
249 Omitting the BirA plasmid from the transfection eliminated the binding of pm142 or

250 pm143 to the AV beads (lane 4). Note that the biotinylation signal caused a slight but
251 detectable increase in the size of the pm142 and pm143 proteins (compare lanes 2 and 3).

252 Immunoblot assays of the same samples using PKR antiserum revealed that at
253 least a small amount of PKR was precipitated by the pm142:pm143 complex and by
254 pm142 and pm143 individually (Fig 2B, lanes 2, 3, 5, and 6). pTRS1-B-H also
255 precipitated PKR (lane 1), consistent with our previous finding that pTRS1 binds to PKR
256 (11). As expected, the negative controls (samples lacking BirA or pulled down with
257 EGFP-B-H) did not precipitate PKR (lanes 4, 7 and 8). Treatment of the
258 immunoprecipitated material with dsRNA-specific RNase (RNaseIII) under conditions
259 that completely digested reovirus genomic dsRNA, did not disrupt the association of
260 pm143 with pm142 or with PKR (data not shown). However, dsRNA that is embedded in
261 the complex might not be accessible to the RNaseIII, so these results do not exclude the
262 possibility that dsRNA is a key component of the complex. However, these data do
263 reveal that pm142 and pm143 each appear to bind to PKR independently.

264

265 **Expression of pm142 stabilizes pm143.** We noticed that the abundance of pm143 in
266 lysates was consistently much lower when it was expressed by itself or with EGFP than
267 when expressed with pm142 (e.g. compare lanes 6 and 8 to lanes 2, 3, and 4 in Fig. 2A,
268 top panel). To evaluate the possibility that pm143 might be stabilized by its association
269 with pm142, we measured the half-life of pm143 in cells transfected with pm143-B-H in
270 the presence or absence of pm142-H (Fig. 3). At 24 h post-transfection, we pulse-labeled
271 cells with [³⁵S]-methionine for 1 h, then chased with excess cold methionine and
272 analyzed proteins bound to AV-agarose by electrophoresis and phosphorimager analysis.

273 As is evident in Fig. 3, even by two hours post-chase there was substantially less pm143
274 in the absence of pm142 than when the proteins were co-expressed. The calculated half-
275 life of pm143 was approximately 8 h in the absence of pm142 and 25 h when expressed
276 in combination with pm142. Thus, pm143 is stabilized by coexpression of pm142.

277

278 **The pm142:pm143 complex is larger than a heterodimer but lacks substantial**
279 **amounts of PKR.** The observation that pm142 and pm143 bind to each other and that
280 both also bind to PKR (Figs. 1 and 2) suggested that these three proteins might form a
281 heterotrimeric complex in infected cells. To test this hypothesis, we fractionated infected
282 cell lysates over glycerol gradients and analyzed the distribution of these three proteins
283 by SDS-PAGE and immunoblot assays (Fig. 4). In parallel gradients, we fractionated
284 molecular weight standards in an identical manner and determined their distribution by
285 polyacrylamide gel electrophoresis and Coomassie Blue staining.

286 Most of the pm143 migrated with a peak of pm142 at an apparent size of ~200
287 kDa (Fig. 4A, fractions 12 - 17), which is close to the calculated size (178 kDa) of a
288 heterotrimer consisting of one molecular each of pm142 (49 kDa), pm143 (61 kDa) and
289 PKR (68 kDa). Surprisingly, we detected little or no PKR in the fractions containing the
290 pm142:pm143 complex (Fig 4B). Instead, PKR migrated mostly in the range of ~70 kDa
291 to ~160 kDa (fractions 17 - 24). The smaller size within this range corresponds to that
292 of the PKR monomer (68 kDa), while the larger species could represent PKR dimers or
293 PKR bound to other factors. Although the small amount of overlap between pm142,
294 pm143, and PKR (fractions 16-18) might represent PKR:pm142:pm143 heterotrimers,
295 these results indicate that the majority of the pm142:pm143 complex in infected cells is

296 not bound to PKR. Conversely, most of the PKR in the cell appears not to be bound to
297 the pm142:pm143 complex, which may explain the low amount of PKR associating with
298 pm142 and pm143 in our immunoprecipitation experiments (Figs. 1 and 2). However,
299 these data do not exclude the possibility that there is a PKR:pm142:pm143 trimeric
300 complex in infected cells but that it dissociates under the conditions of these experiments.

301 In addition to its presence in the pm142:pm143 complexes, pm142 migrates as a
302 smaller species, possibly representing pm142 monomers and homodimers (see below), as
303 well as in larger complexes of unknown composition. Perhaps due to its labile nature in
304 the absence of pm142 (Fig. 3), pm143 is present only in fractions containing pm142.

305 These results, suggesting that there is a stable ~200 kDa complex consisting of
306 pm142 and pm143 that lacks substantial amounts of PKR, raise two questions. First,
307 what is the composition of the ~200 kDa complex? Second, can we reconcile the
308 observations that pm142 and pm143 can each bind to PKR and prevent its activation yet
309 most of the PKR in the cells appears not to be stably associated with pm142 and pm143?
310 The subsequent studies were designed to evaluate these issues.

311

312 **The pm142:pm143 complex lacks other proteins.** Since the pm142:pm143 complex
313 migrated at a size of ~200 kDa (Fig. 4) and a heterodimer of the two proteins would be
314 expected to be only ~110 kDa, we investigated the possibility that the complex contains
315 additional proteins. First, we transfected cells with plasmids expressing pm142-B-H and
316 pm143-B-H, and at 24 h post-transfection prepared cytoplasmic lysates and analyzed the
317 distribution of the proteins by glycerol gradient centrifugation. Detection of the two
318 transfected proteins using avidin-AP demonstrated that, similar to the complex present in

319 infected cells, the pm142:pm143 multimer sedimented as a ~200 kDa complex in these
320 transfected, uninfected cells (Fig. 5). This result demonstrates that no other MCMV
321 proteins are required for formation of the major pm142:pm143 complex.

322 To evaluate whether any cellular proteins were present in the pm142:pm143
323 multimer, we transfected cells with pm142-H and pm143-B-H and pulled-down pm143-
324 B-H and any associated proteins by binding to AV-agarose. We then detected these
325 proteins by gel electrophoresis followed by silver staining. As a negative control we
326 analyzed lysates from cells transfected with pm142-H and pm143-H, both lacking the
327 biotinylation signal. For comparison, we also analyzed HCMV pTRS1-H-B. Consistent
328 with prior evaluations using immunoblot assays, pm142 was detectable in the pm143-
329 bound material (Fig. 6). Although there were several other minor protein bands, some of
330 which also were detected in the negative control sample, none approached the abundance
331 of the bands corresponding to pm142 and pm143. Thus, the relatively large size of the
332 pm142:pm143 multimer cannot easily be explained by the presence of either additional
333 MCMV or cellular proteins.

334

335 **The pm142:pm143 complex may be a heterotetramer.** The absence of other proteins
336 in the pm142:pm143 complex might be explained by its being a higher order multimer of
337 just these two proteins. To investigate this possibility, we again transfected various
338 plasmids expressing proteins tagged with either His or the biotinylation signal into HeLa
339 cells and assayed total and AV-bound proteins using either anti-His antibody or avidin-
340 AP.

341 When expressed by itself, pm142-B was detectable in lysates and the AV-bound
342 samples using avidin-AP, but not with anti-His (Fig. 7, panels A-D, lanes 1). On the
343 other hand, pm142-H was expressed in lysates (A, lane 2), but it lacks the biotin tag and
344 so, as expected, did not bind to AV-agarose (B, lane 2) nor was it detected by avidin-AP
345 (C and D, lanes 2). However, when pm142-B and pm142-H were co-transfected, pm142-
346 H was pulled down by AV beads (B, lane 3), demonstrating that pm142-H binds to
347 pm142-B, thus suggesting that pm142 can homodimerize.

348 Consistent with its relative instability in the absence of pm142 (Fig. 3), pm143-B
349 transfection by itself resulted in only a faint band in both the lysates and bound fractions
350 (C and D, lanes 4). On an exposure comparable to that shown in panels C and D, pm143-
351 H was almost undetectable (not shown) but with a longer exposure it was clearly present
352 (A, lane 5). In lysates prepared after transfection of both pm143-B and pm143-H, we
353 could detect both proteins in the lysates but only pm143-B in the bound fraction. The
354 observation that all of the other proteins shown Fig. 7 that bound directly or indirectly to
355 AV beads produced bands that appeared at least as intense in bound samples as in the
356 lysates, coupled with the detection of pm143-H in the lysates but not the bound samples,
357 suggests that pm143 does not self-associate.

358 Interestingly, when pm142-H was expressed along with pm143-B and pm143-H,
359 pm143-H was present in the bound fraction along with pm142-H (Fig. 7B, lane 7). This
360 result indicates that pm143-B and pm143-H were tethered together by one or more
361 molecules of pm142. The absence of detectable pm142-H or pm143-H binding to the
362 EGFP-B-H control (lane 8, B) supports the specificity of the binding reactions.

363 Collectively, the results of Figs. 3-6 suggest that the major form of the
364 pm142:pm143 complex is a heterotetramer in which two pm142 molecules bind to each
365 other in addition to each binding to separate pm143 monomers.

366

367 **MCMV causes relocalization of PKR.** We previously reported that pTRS1 and pIRS1
368 not only bind to PKR, but that they also cause accumulation of PKR in the nucleus (11).
369 Because of the similarities between HCMV and MCMV, we hypothesized that MCMV
370 infection might also cause PKR relocalization. To test this idea, we prepared nuclear-
371 and cytoplasmic-enriched fractions of mock- or MCMV-infected NIH 3T3 cells at 24, 48,
372 and 72 h post-infection and evaluated the distribution of PKR by immunoblot analysis
373 (Fig. 8). PKR remained relatively constant in abundance and remained predominantly
374 cytoplasmic during this time interval in mock-infected cells. In contrast, its abundance
375 increased and it redistributed to the nuclear fraction in MCMV-infected cells. We
376 performed control immunoblots on the same cytoplasmic and nuclear extracts to evaluate
377 the efficacy of the fractionation procedure. Antibodies directed against the nuclear
378 marker lamin A/C revealed its presence exclusively in the nuclear fraction. The
379 cytoplasmic marker calnexin was upregulated by MCMV infection, but remained
380 predominantly cytoplasmic in the infected cells. An anti- β -actin immunoblot showed that
381 the abundance of β -actin was similar in mock-infected and infected cells, although it
382 appeared to be slightly more concentrated in the nuclear than the cytoplasmic fractions in
383 both cases. The same extracts were also probed with a mixture of anti-m142 and anti-
384 m143 antisera, and as reported by Hanson et al. (12), pm142 and pm143 were present in
385 both the cytoplasmic and nuclear fractions throughout infection.

386 As a complementary method for assessing the effects of MCMV on PKR, we
387 examined the distribution of PKR in mock- and MCMV-infected cells by indirect
388 immunofluorescence using an Olympus DeltaVision microscope as described in
389 Materials and Methods. In mock-infected NIH 3T3 cells (Fig. 9, panel A), incubation
390 with anti-PKR antibody showed the predominantly cytoplasmic localization of PKR with
391 a small amount of nuclear PKR appearing to localize in the nucleoli, as has been reported
392 by others (14, 15) and consistent with our immunoblot data (Fig. 8). At 48 h post
393 infection, PKR expression was elevated in MCMV-infected cells and a substantially
394 higher amount was detectable in the nucleus. Surprisingly, contrary to the results based
395 on cell fractionation methods (Fig. 8), the majority of the PKR in the infected cells
396 appeared to remain localized within the cytoplasm. The PKR signal in infected cells also
397 seemed distributed in a coarser punctate pattern in the cytoplasm of infected cells
398 compared to mock-infected cells. Staining with an isotype-matched control antibody
399 showed minimal background staining in these cells. As an additional control, we
400 incubated mock- or MCMV-infected PKR-null MEFs with anti-PKR antiserum or the
401 isotype-matched control antibody (Fig. 9B). In these cells, both the anti-PKR and control
402 antibodies revealed only a low level of background fluorescence.

403 Thus, the results of the immunoblot assays and immunofluorescence assays both
404 revealed an increase in the amount of nuclear PKR after MCMV infection. Compared to
405 the immunoblot assays, the immunofluorescence studies indicate that there is more
406 abundant PKR in the cytoplasm at late times post infection. These results suggest that
407 MCMV infection results in relocalization of PKR to both the nucleus and to insoluble
408 cytoplasmic complexes.

409

410 **DISCUSSION**

411 The importance of PKR as a mediator of intracellular innate defenses against viral
412 infections is highlighted by the remarkable number and diversity of viral factors and
413 mechanisms that have evolved to counteract its inhibitory effects on host cell translation
414 (22). In several viral systems, mutants lacking anti-PKR factors are severely attenuated
415 for growth in cell culture and have extremely reduced virulence in animal models.
416 Moreover, the replication defect of some of these viruses has been shown to be reversed
417 at least in part in PKR-deficient cells and, in the case of herpes simplex type-1, even in
418 animals, thus providing genetic support for the functional importance of the interactions
419 between PKR and viral antagonists (19, 30, 31).

420 Many viruses encode a dsRNA-binding protein that can inhibit the PKR pathway.
421 Some viruses, including vaccinia virus, herpes simplex type 1 and HCMV, have been
422 shown to contain a second gene that also inhibits the PKR pathway (4, 6, 16, 22, 26). In
423 these examples, the two genes act independently and, in the vaccinia virus and herpes
424 simplex type 1 cases, at different steps in the PKR activation pathway. The two HCMV
425 genes are very closely related and likely act at the same step. MCMV also has two anti-
426 PKR genes but is unusual in that the two genes act together as a single functional unit.
427 Both m142 and m143 are required for effective dsRNA binding and for rescue of
428 VV Δ E3L replication (7). Furthermore, deletion of either gene results in phosphorylation
429 of PKR and eIF2 α , repression of protein synthesis in infected cells, and eliminates
430 MCMV replication (27). The genomic proximity of m142 and m143 combined with their
431 functional similarities suggest that evolution of MCMV may have resulted in separation

432 of the functions needed for blocking PKR into two proteins, while in other viruses these
433 functions are combined in a single protein.

434 Many well-studied viral dsRNA-binding proteins that prevent PKR activation
435 bind to PKR (4, 11, 20, 24). We found that the pm142:pm143 complex does so as well
436 (Fig. 1). The observation that pm142 and pm143 can each bind to PKR in transfection
437 assays (Fig. 2) argues against the possibility that the separation of dsRNA-binding
438 protein functions in MCMV led to one protein becoming specialized in binding to PKR.
439 We do not know whether the interactions between pm142:pm143 and PKR are direct
440 ones. Data showing that pm142 and pm143 are each able to bind to PKR, yet the
441 combination of both is required for strong binding to dsRNA (7), suggest that a dsRNA
442 tether is not required for PKR binding to pm142 or pm143, but it remains possible that
443 there are other proteins or nucleic acids contributing to the interaction.

444 We also do not yet know whether binding to PKR is required for pm142:pm143
445 function, although based on studies of other viral dsRNA-binding proteins we suspect
446 that it is. HCMV pTRS1 (and pIRS1) and influenza NS1 bind to PKR, and these
447 interactions appear to be essential for its inhibition (12, 20). In the case of vaccinia virus
448 E3L, the C-terminal dsRNA binding domain, in the absence of the N-terminal PKR-
449 binding domain, is sufficient for viral replication in many cell types but it is required for
450 preventing PKR activation late in infection (18), for blocking the inhibitory effects of
451 PKR in a yeast growth assay (24), and for virulence in animal models (3). Evaluating
452 whether E3L function requires it to bind to PKR is complicated by the presence of other
453 functions, including an N-terminal Z-DNA binding domain that may be responsible for
454 some of the observed phenotypes (17). Adding to the complexity, binding to PKR does

455 not always inhibit PKR function, as is clearly illustrated by the activation of PKR
456 resulting from its interaction with the cellular regulator PACT (21). Nonetheless, the fact
457 that both pm142 and pm143 associate with and inhibit PKR does suggest that this is a
458 functionally important physical interaction.

459 The observed binding of pm142, pm143 and PKR to each other in each binary
460 combination suggested that these three proteins might form a heterotrimeric complex.
461 Although we found clear evidence for a complex of pm142 and pm143 in infected or
462 transfected cells, little if any PKR co-migrated with the pm142:pm143 complex. One
463 possible explanation for the observed interaction between PKR and pm142:pm143 by
464 coimmunoprecipitation but not by glycerol gradient fractionation is that the interaction is
465 unstable and therefore the complex dissociated under the conditions used in the glycerol
466 gradient experiments. Alternatively, the interaction might be a transient one, possibly
467 resulting in inactivation of PKR by a mechanism that does not require continued
468 association with the MCMV proteins.

469 We also discovered that MCMV alters the distribution of PKR in infected cells.
470 Our analyses of uninfected cells are consistent with reports indicating that approximately
471 20% of the cellular PKR is present in the nucleus, usually in association with the
472 nucleolus (14, 15). Fractionating cells with detergent revealed accumulation of PKR in
473 the nuclear-enriched pellet fraction by 24 h post infection (Fig.8). Since such pellet
474 fractions may also contain insoluble cytoplasmic material, complementary methods are
475 important for evaluating protein distribution. Using immunofluorescence assays, we
476 found that PKR did indeed appear to accumulate in the nucleus during infection, but a
477 large fraction of it remained in the cytoplasm. PKR accumulates in the nucleus after

478 HCMV infection but not after vaccinia infection (11). Using recombinant vaccinia
479 viruses, we showed that pTRS1 or pIRS1 could mediate this relocalization, suggesting
480 that pm142 and pm143 are plausible candidates for instigating the redistribution of PKR
481 during MCMV infection.

482 Altered distribution of PKR has been reported in other settings. ER stress can
483 cause PKR to accumulate in the nucleus (23). Activated PKR was recently shown to be
484 enriched in the nucleus of high risk myelodysplastic syndrome lymphoblasts (9) and in
485 neurons expressing the human immunodeficiency virus type I gp120 where it may
486 contribute to neurodegeneration (1). Human papilloma virus causes PKR to relocalize
487 both to the nucleus and to cytoplasmic P bodies (13). At present, the role of nuclear
488 accumulation of PKR in infected cells is unknown, but it might serve to keep PKR away
489 from its cytoplasmic targets, or alternatively, to enable interaction with a nuclear target
490 and enhance viral replication. The relocalization of PKR into insoluble cytoplasmic
491 compartments might represent another mechanism for ensuring PKR is sequestered away
492 from translational machinery. Note that our glycerol gradient experiments would not
493 have detected nuclear or insoluble cytoplasmic complexes since these were removed
494 during processing, so it remains possible that pm142 and pm143 are associated with PKR
495 in these sites. Consistent with this possibility, Hanson et al. found that pm142 and
496 pm143 appear to be primarily cytoplasmic by immunofluorescence, but were present in
497 the “nuclear” fractions as well when analyzed by cell fractionation and immunoblot assay
498 (12).

499 Our data suggest that pm142 and pm143 form a stable complex, likely a
500 heterotetramer, consisting of two molecules of pm142 associated with each other and

501 each one associating with a molecule of pm143 (Fig 10). Data supporting this proposed
502 structure include the observations that in infected cells, pm142 and pm143 (i) colocalize
503 by immunofluorescence (12), (ii) coimmunoprecipitate (Fig. 1 and (7)), and (iii) migrate
504 through glycerol gradients as a complex having a size consistent with a heterotetramer
505 (Fig. 4). Further evidence comes from transfection assays showing that (iv) pm143
506 stability requires pm142, (v) the molarity of the two proteins in the complex is similar
507 (based on experiments in which their relative amounts can be compared, as in Figs. 2A,
508 Fig. 5, and Fig. 6) and (vi) pm142 can self-associate while pm143 appears not to do so
509 (Fig. 7).

510 Based on our results, we propose a model in which pm142 and pm143 form a
511 stable soluble heterotetrameric cytoplasmic complex during infection (Fig. 10). This
512 complex serves as a reservoir, poised to interact with PKR and dsRNA. As has been
513 proposed for the mechanism by which E3L functions, the pm142:pm143 complex may
514 associate with PKR and prevent its homodimerization (24). The absence of a stable
515 soluble pm142:pm143:PKR complex may result from its relocalization to the nucleus and
516 insoluble cytoplasmic fractions where PKR would be unable to shut off translation,
517 although it is also possible that a transient interaction with pm142 and pm143 is sufficient
518 to cause PKR to relocalize. Although we do not yet understand the significance of the
519 separation of PKR inhibitory function into two proteins in MCMV, this organization is
520 unique among viruses studied thus far, and we expect that further exploration of this
521 system will help uncover fundamentals of the mechanisms by which dsRNA-binding
522 proteins interfere with PKR function and enable viral replication.

523

524 **ACKNOWLEDGMENTS**

525 We thank Bryan Williams (Cleveland Clinic Foundation) for providing PKR-null MEFs,
526 Laura Hanson and Ann Campbell (Eastern Virginia Medical School) for providing
527 antisera, Bruce Clurman (Fred Hutchinson Cancer Research Center) for the BirA
528 expression plasmid and the Fred Hutchinson Cancer Research Center Scientific Imaging
529 and Genomics Cores for technical assistance. This work was supported by NIH grant
530 AI26672.

531

532

533 **REFERENCES**

- 534 1. **Alirezaei, M., D. D. Watry, C. F. Flynn, W. B. Kiosses, E. Masliah, B. R.**
535 **Williams, M. Kaul, S. A. Lipton, and H. S. Fox.** 2007. Human
536 immunodeficiency virus-1/surface glycoprotein 120 induces apoptosis through
537 RNA-activated protein kinase signaling in neurons. *J Neurosci* **27**:11047-55.
- 538 2. **Beckett, D., E. Kovaleva, and P. J. Schatz.** 1999. A minimal peptide substrate in
539 biotin holoenzyme synthetase-catalyzed biotinylation. *Protein Sci* **8**:921-9.
- 540 3. **Brandt, T. A., and B. L. Jacobs.** 2001. Both carboxy- and amino-terminal
541 domains of the vaccinia virus interferon resistance gene, E3L, are required for
542 pathogenesis in a mouse model. *J Virol* **75**:850-6.
- 543 4. **Cassady, K. A., M. Gross, and B. Roizman.** 1998. The herpes simplex virus
544 US11 protein effectively compensates for the gamma1(34.5) gene if present
545 before activation of protein kinase R by precluding its phosphorylation and that of
546 the alpha subunit of eukaryotic translation initiation factor 2. *J Virol* **72**:8620-6.
- 547 5. **Chang, H. W., L. H. Uribe, and B. L. Jacobs.** 1995. Rescue of vaccinia virus
548 lacking the E3L gene by mutants of E3L. *J Virol* **69**:6605-8.
- 549 6. **Child, S. J., M. Hakki, K. L. De Niro, and A. P. Geballe.** 2004. Evasion of
550 cellular antiviral responses by human cytomegalovirus TRS1 and IRS1. *J Virol*
551 **78**:197-205.

- 552 7. **Child, S. J., L. K. Hanson, C. E. Brown, D. M. Janzen, and A. P. Geballe.**
553 2006. Double-stranded RNA binding by a heterodimeric complex of murine
554 cytomegalovirus m142 and m143 proteins. *J Virol* **80**:10173-80.
- 555 8. **Dever, T. E., A. C. Dar, and F. Sicheri.** 2007. The eIF2alpha kinases, p. 319-
556 344. *In* M. B. Matthews, N. Sonenberg, and J. W. B. Hershey (ed.), *Translational*
557 *Control in Biology and Medicine*. Cold Spring Harbor Press.
- 558 9. **Follo, M. Y., C. Finelli, S. Mongiorgi, C. Clissa, C. Bosi, G. Martinelli, W. L.**
559 **Blalock, L. Cocco, and A. M. Martelli.** 2008. PKR is activated in MDS patients
560 and its subcellular localization depends on disease severity. *Leukemia*.
- 561 10. **Hakki, M., and A. P. Geballe.** 2005. Double-stranded RNA binding by human
562 cytomegalovirus pTRS1. *J Virol* **79**:7311-8.
- 563 11. **Hakki, M., E. E. Marshall, K. L. De Niro, and A. P. Geballe.** 2006. Binding
564 and nuclear relocalization of protein kinase R by human cytomegalovirus TRS1. *J*
565 *Virol* **80**:11817-26.
- 566 12. **Hanson, L. K., B. L. Dalton, L. F. Cageao, R. E. Brock, J. S. Slater, J. A.**
567 **Kerry, and A. E. Campbell.** 2005. Characterization and regulation of essential
568 murine cytomegalovirus genes m142 and m143. *Virology* **334**:166-77.
- 569 13. **Hebner, C. M., R. Wilson, J. Rader, M. Bidder, and L. A. Laimins.** 2006.
570 Human papillomaviruses target the double-stranded RNA protein kinase pathway.
571 *J Gen Virol* **87**:3183-93.
- 572 14. **Jeffrey, I. W., S. Kadereit, E. F. Meurs, T. Metzger, M. Bachmann, M.**
573 **Schwemmler, A. G. Hovanessian, and M. J. Clemens.** 1995. Nuclear

- 574 localization of the interferon-inducible protein kinase PKR in human cells and
575 transfected mouse cells. *Exp Cell Res* **218**:17-27.
- 576 15. **Jimenez-Garcia, L. F., S. R. Green, M. B. Mathews, and D. L. Spector.** 1993.
577 Organization of the double-stranded RNA-activated protein kinase DAI and virus-
578 associated VA RNAI in adenovirus-2-infected HeLa cells. *J Cell Sci* **106 (Pt**
579 **1)**:11-22.
- 580 16. **Khoo, D., C. Perez, and I. Mohr.** 2002. Characterization of RNA determinants
581 recognized by the arginine- and proline-rich region of Us11, a herpes simplex
582 virus type 1-encoded double-stranded RNA binding protein that prevents PKR
583 activation. *J Virol* **76**:11971-81.
- 584 17. **Kim, Y. G., M. Muralinath, T. Brandt, M. Pearcy, K. Hauns, K.**
585 **Lowenhaupt, B. L. Jacobs, and A. Rich.** 2003. A role for Z-DNA binding in
586 vaccinia virus pathogenesis. *Proc Natl Acad Sci U S A* **100**:6974-9.
- 587 18. **Langland, J. O., and B. L. Jacobs.** 2004. Inhibition of PKR by vaccinia virus:
588 role of the N- and C-terminal domains of E3L. *Virology* **324**:419-29.
- 589 19. **Leib, D. A., M. A. Machalek, B. R. Williams, R. H. Silverman, and H. W.**
590 **Virgin.** 2000. Specific phenotypic restoration of an attenuated virus by knockout
591 of a host resistance gene. *Proc Natl Acad Sci U S A* **97**:6097-101.
- 592 20. **Li, S., J. Y. Min, R. M. Krug, and G. C. Sen.** 2006. Binding of the influenza A
593 virus NS1 protein to PKR mediates the inhibition of its activation by either PACT
594 or double-stranded RNA. *Virology* **349**:13-21.

- 595 21. **Li, S., G. A. Peters, K. Ding, X. Zhang, J. Qin, and G. C. Sen.** 2006. Molecular
596 basis for PKR activation by PACT or dsRNA. *Proc Natl Acad Sci U S A*
597 **103**:10005-10.
- 598 22. **Mohr, I. J., T. Pe'ery, and M. B. Mathews.** 2007. Protein Synthesis and
599 Translational Control during Viral Infection, p. 545-599. *In* M. B. Mathews, N.
600 Sonenberg, and J. W. B. Hershey (ed.), *Translational Control in Biology and*
601 *Medicine*. Cold Spring Harbor Press.
- 602 23. **Onuki, R., Y. Bando, E. Suyama, T. Katayama, H. Kawasaki, T. Baba, M.**
603 **Tohyama, and K. Taira.** 2004. An RNA-dependent protein kinase is involved in
604 tunicamycin-induced apoptosis and Alzheimer's disease. *Embo J* **23**:959-68.
- 605 24. **Romano, P. R., F. Zhang, S. L. Tan, M. T. Garcia-Barrio, M. G. Katze, T. E.**
606 **Dever, and A. G. Hinnebusch.** 1998. Inhibition of double-stranded RNA-
607 dependent protein kinase PKR by vaccinia virus E3: role of complex formation
608 and the E3 N-terminal domain. *Mol Cell Biol* **18**:7304-16.
- 609 25. **Sadler, A. J., and B. R. Williams.** 2008. Interferon-inducible antiviral effectors.
610 *Nat Rev Immunol* **8**:559-68.
- 611 26. **Shors, S. T., E. Beattie, E. Paoletti, J. Tartaglia, and B. L. Jacobs.** 1998. Role
612 of the vaccinia virus E3L and K3L gene products in rescue of VSV and EMCV
613 from the effects of IFN-alpha. *J Interferon Cytokine Res* **18**:721-9.
- 614 27. **Valchanova, R. S., M. Picard-Maureau, M. Budt, and W. Brune.** 2006.
615 Murine cytomegalovirus m142 and m143 are both required to block protein
616 kinase R-mediated shutdown of protein synthesis. *J Virol* **80**:10181-90.

- 617 28. **van Den Pol, A. N., E. Mocarski, N. Saederup, J. Vieira, and T. J. Meier.**
618 1999. Cytomegalovirus cell tropism, replication, and gene transfer in brain. *J*
619 *Neurosci* **19**:10948-65.
- 620 29. **Weber, F., V. Wagner, S. B. Rasmussen, R. Hartmann, and S. R. Paludan.**
621 2006. Double-stranded RNA is produced by positive-strand RNA viruses and
622 DNA viruses but not in detectable amounts by negative-strand RNA viruses. *J*
623 *Virology* **80**:5059-64.
- 624 30. **Xiang, Y., R. C. Condit, S. Vijaysri, B. Jacobs, B. R. Williams, and R. H.**
625 **Silverman.** 2002. Blockade of interferon induction and action by the E3L double-
626 stranded RNA binding proteins of vaccinia virus. *J Virol* **76**:5251-9.
- 627 31. **Zhang, P., B. L. Jacobs, and C. E. Samuel.** 2008. Loss of protein kinase PKR
628 expression in human HeLa cells complements the vaccinia virus E3L deletion
629 mutant phenotype by restoration of viral protein synthesis. *J Virol* **82**:840-8.

630

631 **FIGURE LEGENDS**

632

633 **Figure 1.** The pm142 and pm143 proteins bind PKR in MCMV-infected cells. NIH 3T3
634 cells were mock-infected (lanes 1, 3, 4, and 5) or infected with MCMV (lanes 2, 6, 7 and
635 8; MOI = 3), and at 48 h post-infection lysates were prepared and analyzed by
636 immunoblot assay directly (lanes 1 and 2) or after immunoprecipitation with the
637 preimmune serum (lanes 3 and 6), pm142 antiserum (lanes 4 and 7) or pm143 antiserum
638 (lanes 5 and 8). (A) Unbound mock and infected cell lysates (lanes 1 and 2; 3% of the
639 amount immunoprecipitated) and 20% of each bound sample (lanes 3 – 8) were probed

640 using a mixture of m142 and m143 antisera. The migration of pm142, pm143, and the
641 IgG heavy chain (HC) are indicated on the right. (B) Lysates and the remaining 80% of
642 each bound sample were probed with the anti-PKR antibody.

643

644 **Figure 2.** Both pm142 and pm143 bind to PKR in transfected cells. HeLa cells were
645 transfected with the indicated plasmids, all of which express proteins containing His tags
646 alone (-H) or with a biotinylation signal (-B-H). All transfections, except that in lane 4,
647 also included the plasmid encoding biotin ligase (pSC2+BirA). At 48 h post-transfection
648 cell lysates were prepared and incubated with AV-agarose and analyzed by immunoblot
649 assay as described in Materials and Methods. (A) Membranes with unbound lysates (top
650 panel) or 20% of the bound samples (bottom panel) were probed with the anti-His
651 antibody. (B) Membranes with unbound lysate (top panel) and 80% of the bound
652 samples (lower panel) were subjected to immunoblot analysis with the PKR antibody.

653

654 **Figure 3.** The pm143 protein is stabilized by co-expression of pm142. HeLa cells were
655 transiently transfected with m143-B-H alone or in combination with m142-H. At 24 h
656 post-transfection the cells were pulse labeled with [³⁵S]methionine for 1 h then re-fed
657 with medium containing excess cold methionine. Cell lysates were prepared at the
658 indicated times post-chase and proteins binding to AV-agarose were analyzed by
659 electrophoresis and phosphorimager analysis.

660

661 **Figure 4.** Size fractionation of pm142:pm143 complexes and PKR on glycerol density
662 gradients. NIH 3T3 cells were infected with MCMV (MOI = 3), and at 48 h post-

663 infection cell lysates were prepared and centrifuged through 15-35% glycerol density
664 gradients as described in Materials and Methods. Following centrifugation, fractions
665 were collected from the bottom of the gradients, and the fractions were separated on
666 polyacrylamide gels, transferred to PVDF, and probed with (A) a mixture of m142 and
667 m143 antisera, after which the blot was stripped and re-probed with (B) an anti-PKR
668 antibody. Molecular weight standards were size fractionated on a parallel gradient, then
669 analyzed by polyacrylamide gel electrophoresis and Coomassie blue staining. The
670 migration of the molecular weight standards is indicated below panel B. Note that
671 fractions 5 and 7 were lost during processing and that aliquots of the lysates (lys) prior to
672 fractionation were included in the first and last lanes.

673

674 **Figure 5.** The pm142:pm143 complex does not contain additional MCMV proteins.
675 HeLa cells were transfected with plasmids expressing BirA, m142-B-H and m143-B-H,
676 and at 24 h post-transfection lysates were prepared and fractionated on 15-35% glycerol
677 density gradients as described in Materials and Methods. The indicated subset of
678 fractions were analyzed by gel electrophoresis, transfer to PVDF, and detection of the
679 biotin-tagged pm142 and pm143 proteins using avidin-AP. The migration of molecular
680 weight standards analyzed on a parallel gradient is indicated below.

681

682 **Figure 6.** The pm142:pm143 complex does not include cellular proteins. HeLa cells
683 were transfected with plasmids expressing m143-B-H and m142-H, TRS1-B-H, or m143-
684 H plus m142-H. All samples also included pSC2+BirA. At 48 h post-transfection

685 lysates were prepared and incubated with AV-agarose as described in Materials and
686 Methods, and bound proteins were analyzed by gel electrophoresis and silver staining.

687

688 **Figure 7.** The pm142 and pm143 proteins appear to form a heterotetrameric complex.
689 HeLa cells were transfected with pSC2+BirA in addition to the indicated plasmids that
690 express either His- or biotin-tagged forms of pm142 and pm143. At 48 h post-
691 transfection lysates were collected, incubated with avidin-agarose, and subjected to
692 immunoblot analysis as previously described. Membranes containing (A) unbound
693 lysates (3% of total) and (B) 50% of the bound samples (bottom panel) were probed with
694 anti-His antibody. Membranes with (C) unbound (3% of total) and (D) bound lysates
695 (50% of total) were probed with avidin-AP to detect biotin-tagged proteins.

696

697 **Figure 8.** MCMV infection causes nuclear relocalization of PKR. NIH 3T3 cells were
698 mock-infected or infected with MCMV (MOI = 3). Cell lysates were prepared at 24, 48,
699 and 72 h post-infection and separated into cytoplasmic- (cyt) and nuclear-enriched (nuc)
700 fractions as described in Materials and Methods. Equal amounts of each fraction were
701 subjected to gel electrophoresis, transferred to PVDF membranes, and probed with the
702 indicated antisera including the nuclear marker lamin A/C and the cytoplasmic marker
703 calnexin.

704

705 **Figure 9.** MCMV infection appears to cause PKR relocalization to both the nucleus and
706 insoluble cytoplasmic complexes. NIH 3T3 and PKR null cells grown on coverslips were
707 mock-infected or infected with MCMV (MOI = 3). At 48 h post-infection the cells were

708 fixed, incubated with anti-PKR or an isotype control antibody, and prepared for
709 immunofluorescence as described in Materials and Methods. Samples were analyzed by
710 deconvolution microscopy.

711

712 **Figure 10.** Model depicting putative mechanisms of PKR inactivation and re-
713 localization by pm142 and pm143. In the absence of viral antagonists (1), PKR is
714 activated by dsRNA, which leads to dimerization, auto-phosphorylation, and subsequent
715 phosphorylation of the alpha subunit of the translation initiation factor eIF2, thereby
716 blocking translation and inhibiting viral replication. During MCMV infection, a stable
717 heterotetrameric pm142:pm143 complex forms which can interact with PKR and dsRNA.
718 (2), Whether or not pm142 and pm143 remain associated with PKR is not yet clear but
719 we hypothesize that these viral proteins cause sequestration of PKR in the nucleus and in
720 insoluble cytoplasmic complexes (gray area) where it is unlikely to be able to shut off
721 translation and block viral replication.

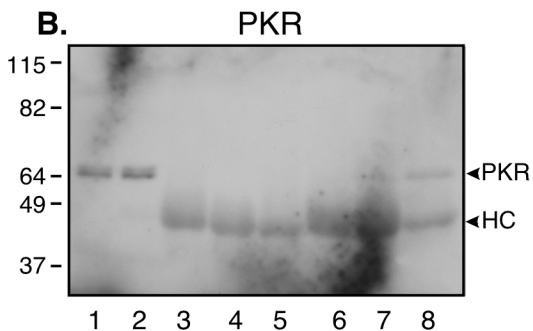
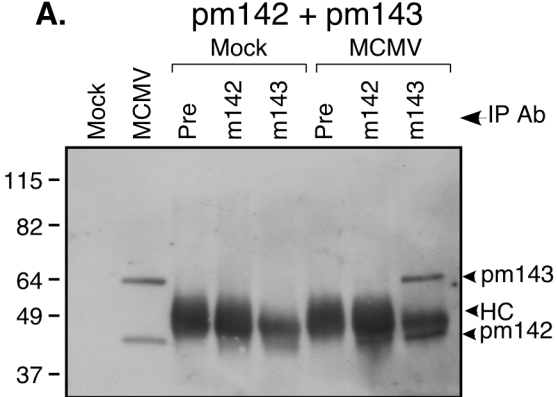


Figure 1

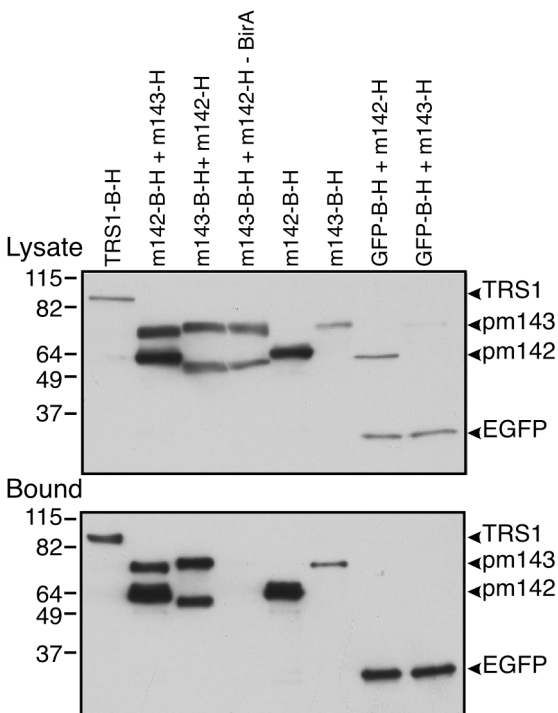
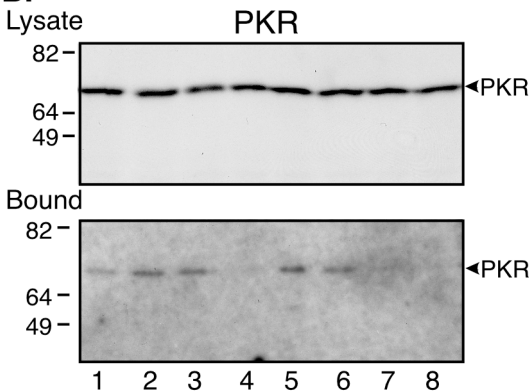
A.**HIS****B.**

Figure 2

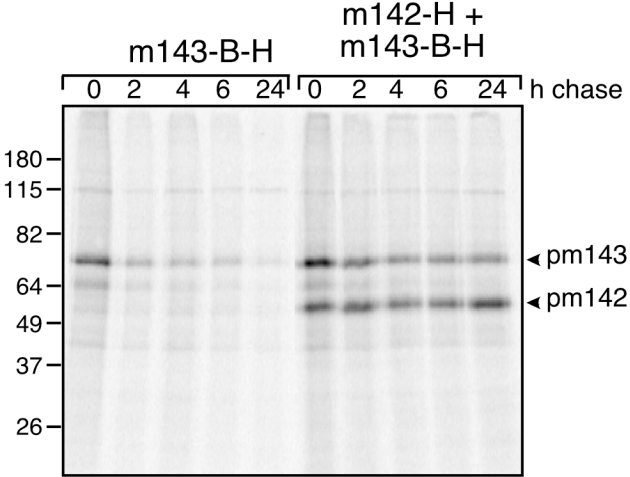


Figure 3

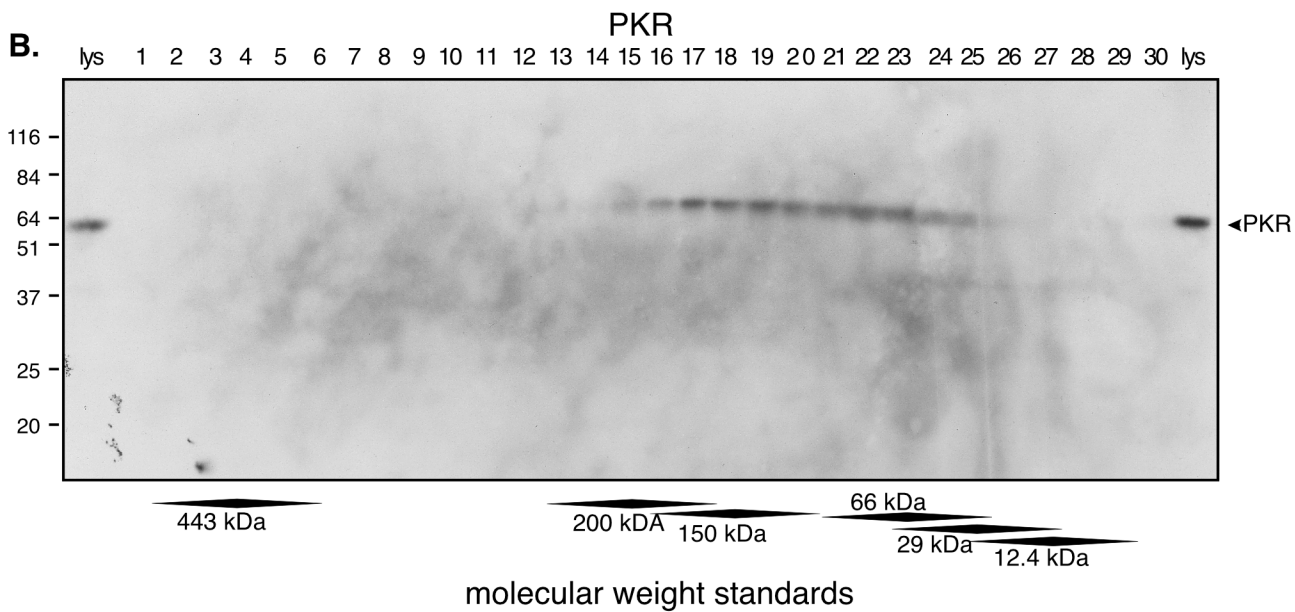
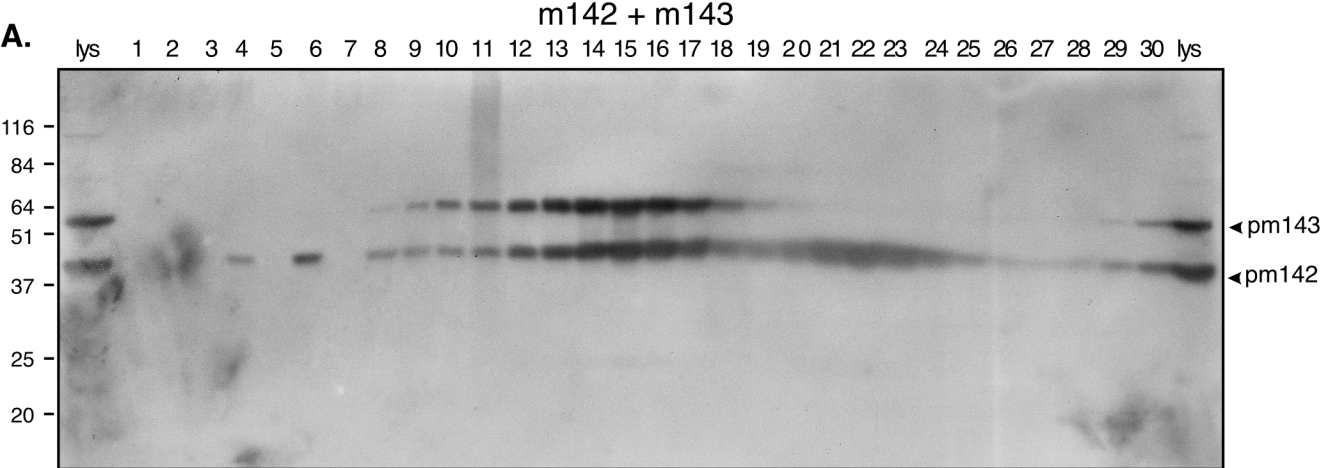


Figure 4

m142 + m143

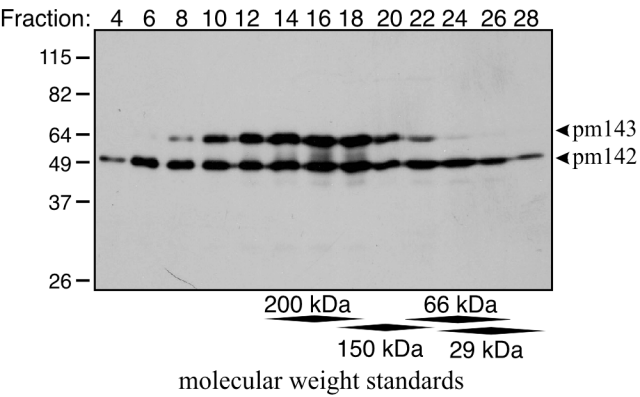


Figure 5

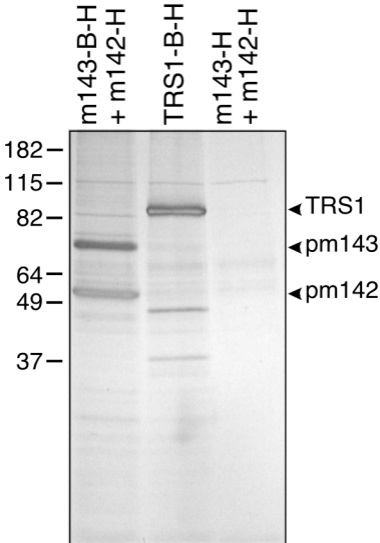


Figure 6

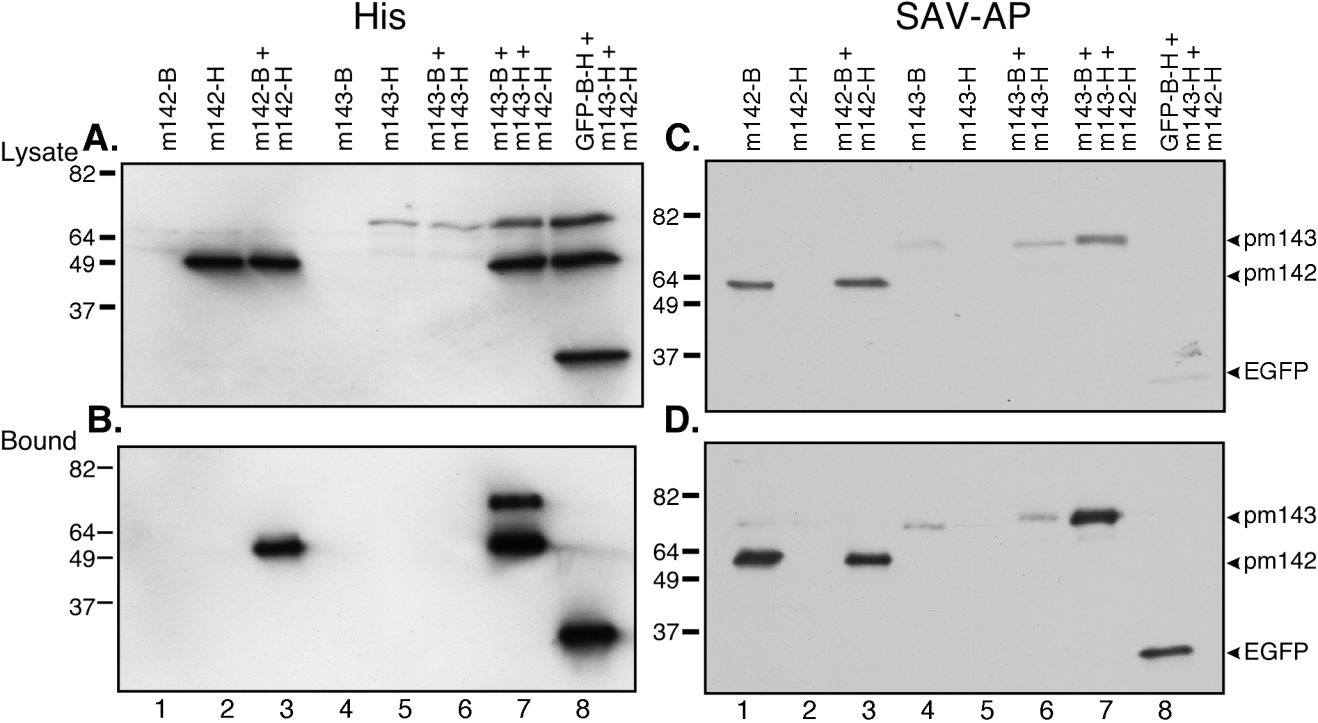


Figure 7

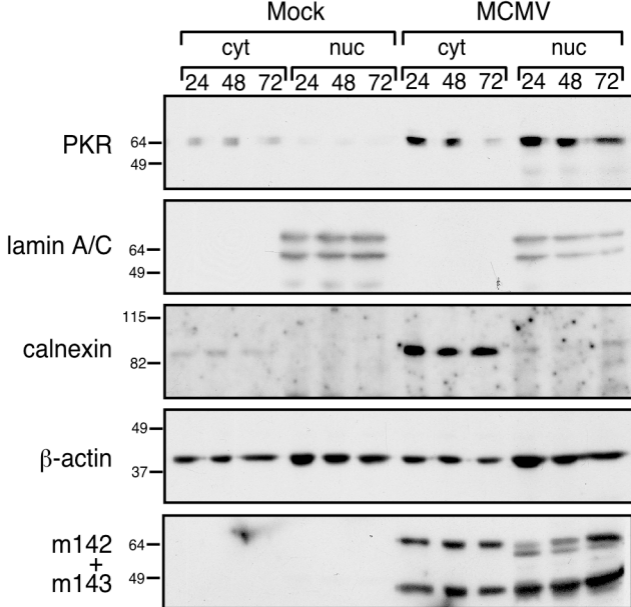


Figure 8

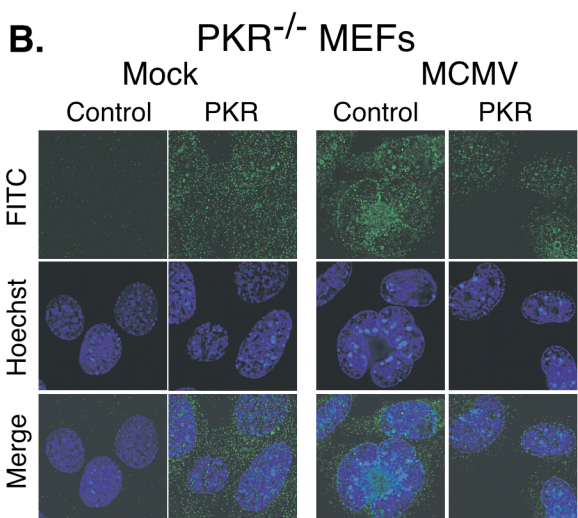
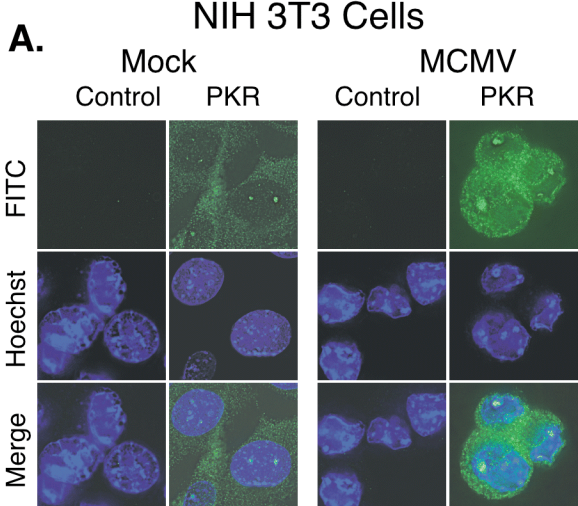


Figure 9

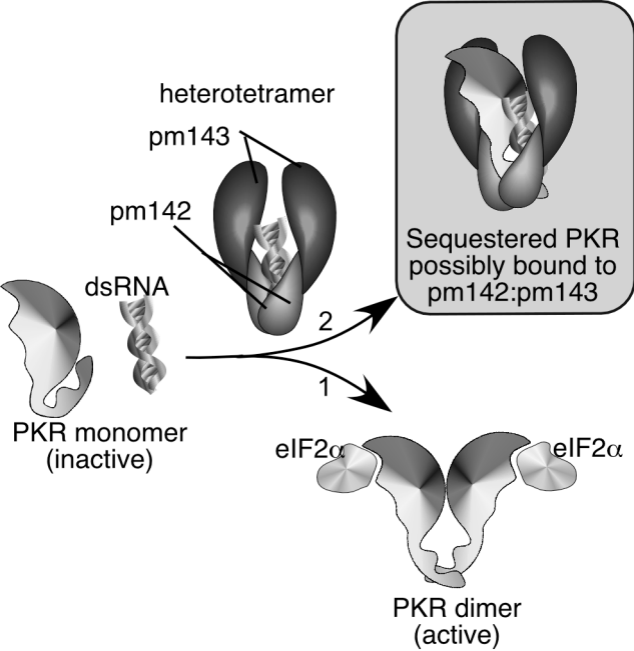


Figure 10